JOURNAL OF MATERIALS SCIENCE 21 (1986) 4131–4139

Deformation behaviour of retained β phase in β-eutectoid Ti–Cr alloys

S. HANADA, O. IZUMI
The Research Institute for Iron, Steel and Other Metals, Tohoku University, Sendai 980, Japan

Plastic deformation mode and its relation to tensile properties were investigated in retained β phase of β-eutectoid type Ti–Cr alloys. A plate-like single variant ω phase is induced during deformation of the most unstable β phase having a minimum chromium content required to suppress martensitic transformation. A selected area electron diffraction pattern taken from a boundary region of the stress-induced ω phase plate can be explained by the idea that a single variant of ω phase is induced in a $\{332\}$ $\langle 113\rangle$ twin produced during deformation. Anisotropy in population of four ω phase variants decreases with increasing chromium content. On further increasing chromium content, deformation occurs by slip. Enhanced ductility is obtained in as-quenched Ti–Cr alloys accompanied by ω phase transformation or $\{332\}$ $\langle 113\rangle$ twinning during deformation. ω phase of as-quenched Ti–Cr alloys changes continuously from commensurate structure with sharp reflections to incommensurate structure with diffuse reflections with increasing chromium content. The obtained results in β-eutectoid type Ti–Cr alloys are quite similar to those in β-isomorphous type Ti–V alloys.

1. Introduction
ω phase formation in β phase titanium alloys is observed to occur either during quenching from the high temperature β phase region or during ageing of quenched alloys. The athermal or aged ω phase has been extensively studied and relatively well characterized both from the standpoint of crystallography and microstructure [1–4], since the microstructure of ω phase significantly influences mechanical or superconducting properties. On the other hand, it has been reported in several β phase titanium alloys that ω phase is also introduced by deformation at room temperature. Brotzen *et al.* [5] found that intensities of ω diffraction lines increased during compressive deformation of a quenched Ti–15 wt % V alloy. Bagaryatskij *et al.* [6] showed that ω phase formed during deformation of a quenched Ti–8 wt % Cr alloy. Kuan *et al.* [7] observed that ω phase was stress-induced during tensile deformation of quenched Ti–16 and Ti–20 wt % V single crystals. Hida *et al.* [8] also found stress-induced ω phase in a quenched Ti–14 wt % Mo single crystal subjected to tensile deformation. On the contrary, Silcock [9] could find no definite effect of deformation in quenched Ti–29 wt % V and Ti–13 wt % Mo alloys. Recently, the present authors [10, 11] have observed ω phase formation during compressive or tensile deformation in quenched Ti–V single crystals with compositions from 16 to 20 wt % V or quenched Ti–Fe single crystals with compositions from 4.5 to 5 wt % Fe, while they have found no ω phase during deformation of quenched Ti–Mo or Ti–Nb single crystals.

The obtained results are conflicting in Ti–Mo alloys, although they are consistent in Ti–V alloys. The discrepancy in Ti–Mo alloys is not clearly understood at present.

This research is part of a study on the correlation between plastic deformation modes and tensile properties in retained β phase titanium alloys. The purpose of the present study is to investigate plastic deformation modes of retained β Ti–Cr alloys as a function of composition in comparison with other β phase titanium alloys. In addition, effect of the determined plastic deformation modes on tensile properties will be discussed.

2. Experimental procedure
Six Ti–Cr alloys containing 8, 10, 11.5, 13, 15 and 20 wt % chromium were prepared by arc melting in a water-cooled copper hearth under an argon atmosphere. The arc melted buttons with a thickness of about 12 mm were hot rolled to 3 mm thick plates at 1073 K and cold rolled to 1.5 mm thick plates. Tensile specimens with dimensions of 3 mm × 1.5 mm × 16 mm and X-ray diffraction samples of 10 mm × 15 mm × 1.5 mm were prepared from the plates and sealed in a quartz tube under a vacuum of 2×10^{-3} Pa. They were homogenized for 14.4 ksec at various temperatures between 1100 and 1150 K to obtain a constant grain size of 0.2 mm and quenched into ice water by breaking the quartz tube immediately after quenching. Plastic deformation modes were determined by optical and transmission electron microscopic observations of fractured or 5% strained tensile specimens and by X-ray diffraction analysis of rolled plates. Stess-induced ω transformation was investigated in a X-ray diffractometer with Mo$K\alpha$ radiation incident to the surface of a rotating specimen.

3. Results
Fig. 1 shows optical micrographs of Ti–Cr alloys rolled by 10% at 300 K after solution treatment.

0022–2461/86 $03.00 + .12

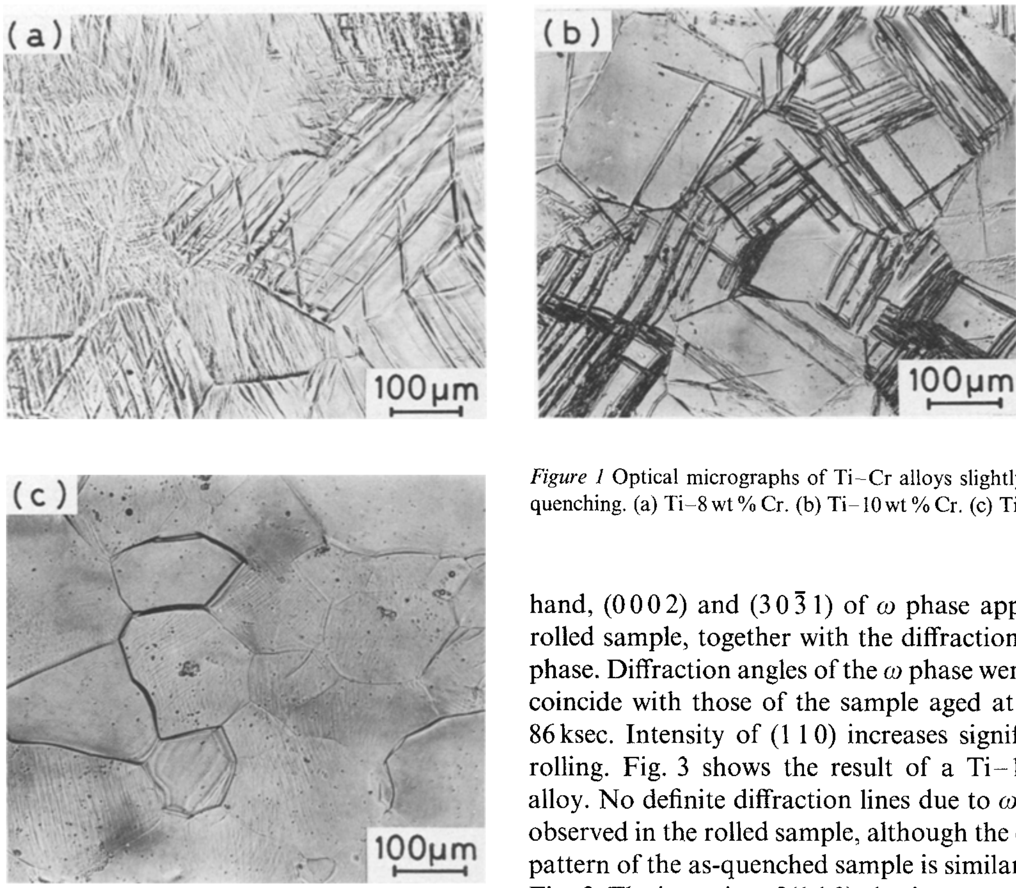

Figure 1 Optical micrographs of Ti–Cr alloys slightly rolled after quenching. (a) Ti–8 wt % Cr. (b) Ti–10 wt % Cr. (c) Ti–13 wt % Cr.

Many straight bands of approximately 10 μm in width are seen in Ti–8 wt % Cr and Ti–10 wt % Cr alloys, while wavy fine markings are visible in a Ti–13 wt % Cr alloy, suggesting that plastic deformation mode is dependent on composition. The mode was determined by X-ray diffraction and transmission electron microscopy. Fig. 2 shows X-ray diffraction patterns of as-quenched and rolled Ti–8 wt % Cr alloys. The rolling was done in reduction of 10% at 300 K. Diffraction lines (1 1 0), (2 0 0) and (2 1 1) of b c c β phase are seen in the as-quenched sample. On the other hand, (0 0 0 2) and (3 0 $\bar{3}$ 1) of ω phase appear in the rolled sample, together with the diffraction lines of β phase. Diffraction angles of the ω phase were found to coincide with those of the sample aged at 573 K for 86 ksec. Intensity of (1 1 0) increases significantly by rolling. Fig. 3 shows the result of a Ti–10 wt % Cr alloy. No definite diffraction lines due to ω phase are observed in the rolled sample, although the diffraction pattern of the as-quenched sample is similar to that of Fig. 2. The intensity of (1 1 0) also increases by rolling. Fig. 4 shows that only diffraction lines of β single phase are observable both in the as-quenched and rolled Ti–13 wt % Cr alloys. (1 1 0) line cannot be seen in the as-quenched condition and it increases slightly by rolling.

Fig. 5a shows selected area electron diffraction patterns taken from a boundary region of a stress-induced product appeared in a tensile specimen of a Ti–10 wt % Cr alloy subjected to 3% plastic strain. Figs 5b and c are taken from β phase matrix adjacent to the boundary region and the product, respectively. Fig. 5d is a key diagram of Fig. 5a. These electron

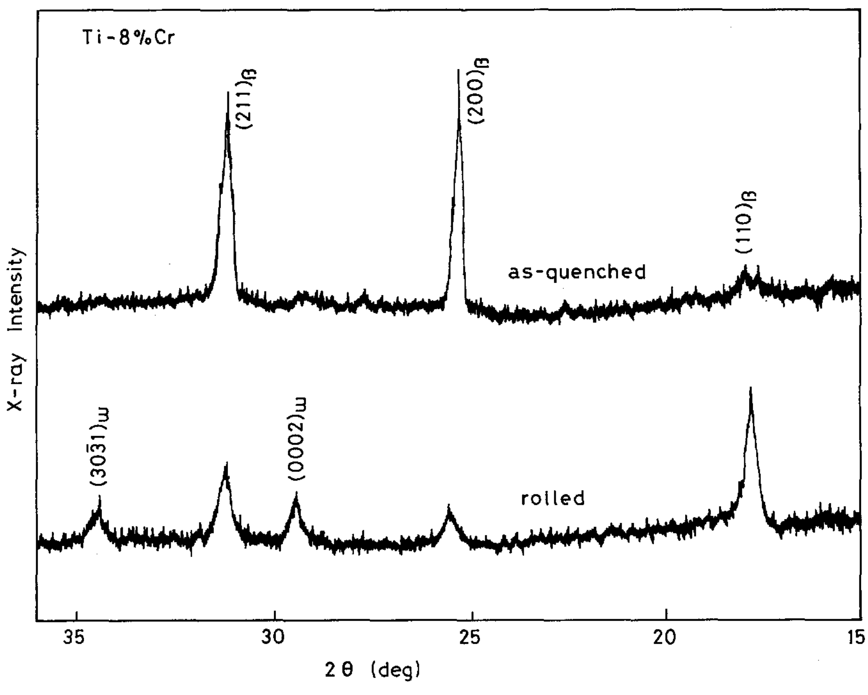

Figure 2 X-ray diffraction patterns of as-quenched and rolled Ti–8 wt % Cr alloys. Rolling was done in reduction of 10% at 300 K.

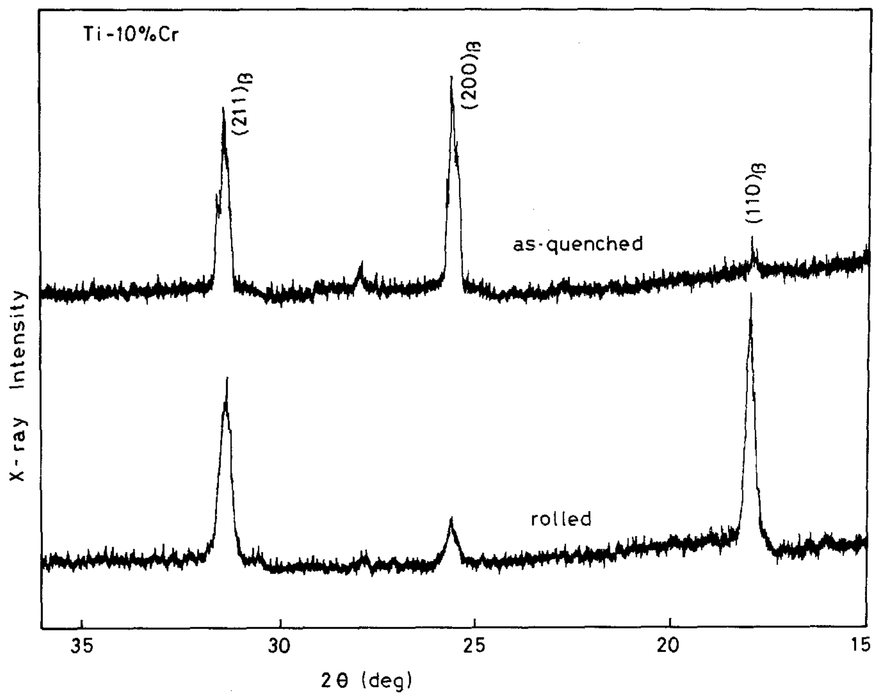

Figure 3 X-ray diffraction patterns of as-quenched and rolled Ti–10 wt % Cr alloys.

diffraction patterns indicate clearly that the stress-induced product is {3 3 2} ⟨1 1 3⟩ twinning, since Fig. 5a can be explained by the key diagram of Fig. 5d. Athermal ω reflections of two variants, ω_1 and ω_2, shows no difference in intensity in the matrix, while there exists anisotropy in the twin. Similar results are obtained in a stress-induced product of a Ti–8 wt % Cr alloy, as shown in Fig. 6, where the anisotropy of ω variants is pronounced. Namely, a single variant of ω phase forms in the twin. Thus, it is considered that stress-induced ω phase via {3 3 2} ⟨1 1 3⟩ twinning occurs on deformation of Ti–8 wt % Cr alloys. In Ti–Cr alloys containing chromium more than 11.5 wt %, no twin was observed, but only dislocations were present after deformation. The obtained composition dependence of the plastic deformation mode in Ti–Cr alloys is in good agreement with that in Ti–V alloys [11]. The deformation mode does not change as plastic strain increases. Fig. 7 shows the optical micrographs of Ti–10 wt % Cr and Ti–13 wt % Cr alloys slightly and heavily deformed in tensile tests. Mechanical twins preferentially appear in the heavily deformed sample as well as the slightly deformed one. Therefore, the present results suggests that tensile properties of β Ti–Cr alloys are significantly influenced by the plastic deformation modes.

Fig. 8 shows the summarized results on tensile properties of β Ti–Cr alloys deformed at 300 K. Tensile properties of the Ti–Cr alloys accompanied by stress-induced ω phase transformation or mechanical twinning are indicated by solid symbols, while those accompanied by slip are illustrated by open symbols. Yield

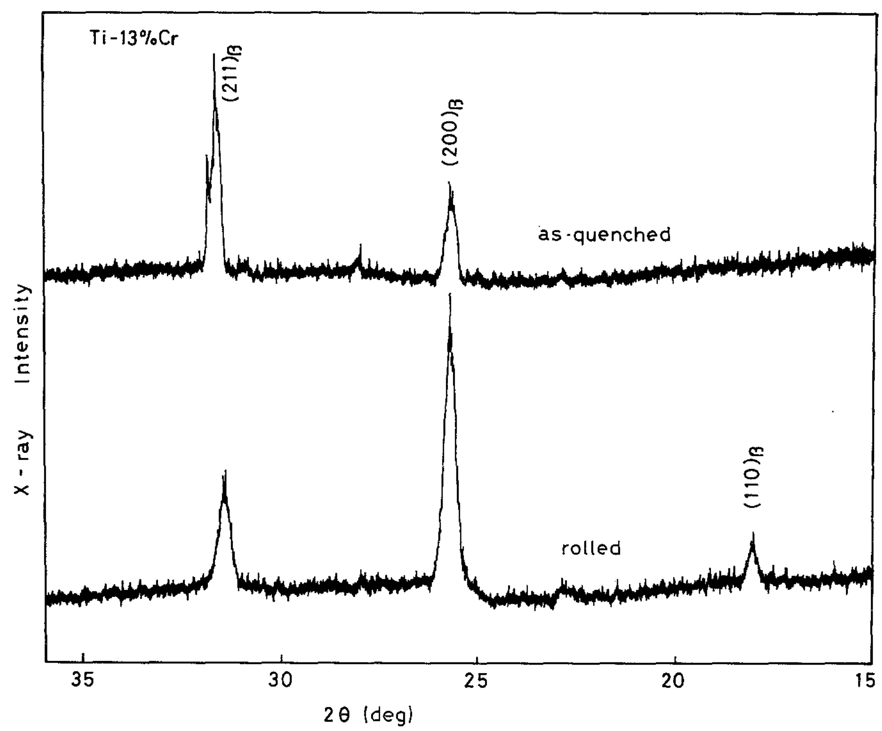

Figure 4 X-ray diffraction patterns of as-quenched and rolled Ti–13 wt % Cr alloys.

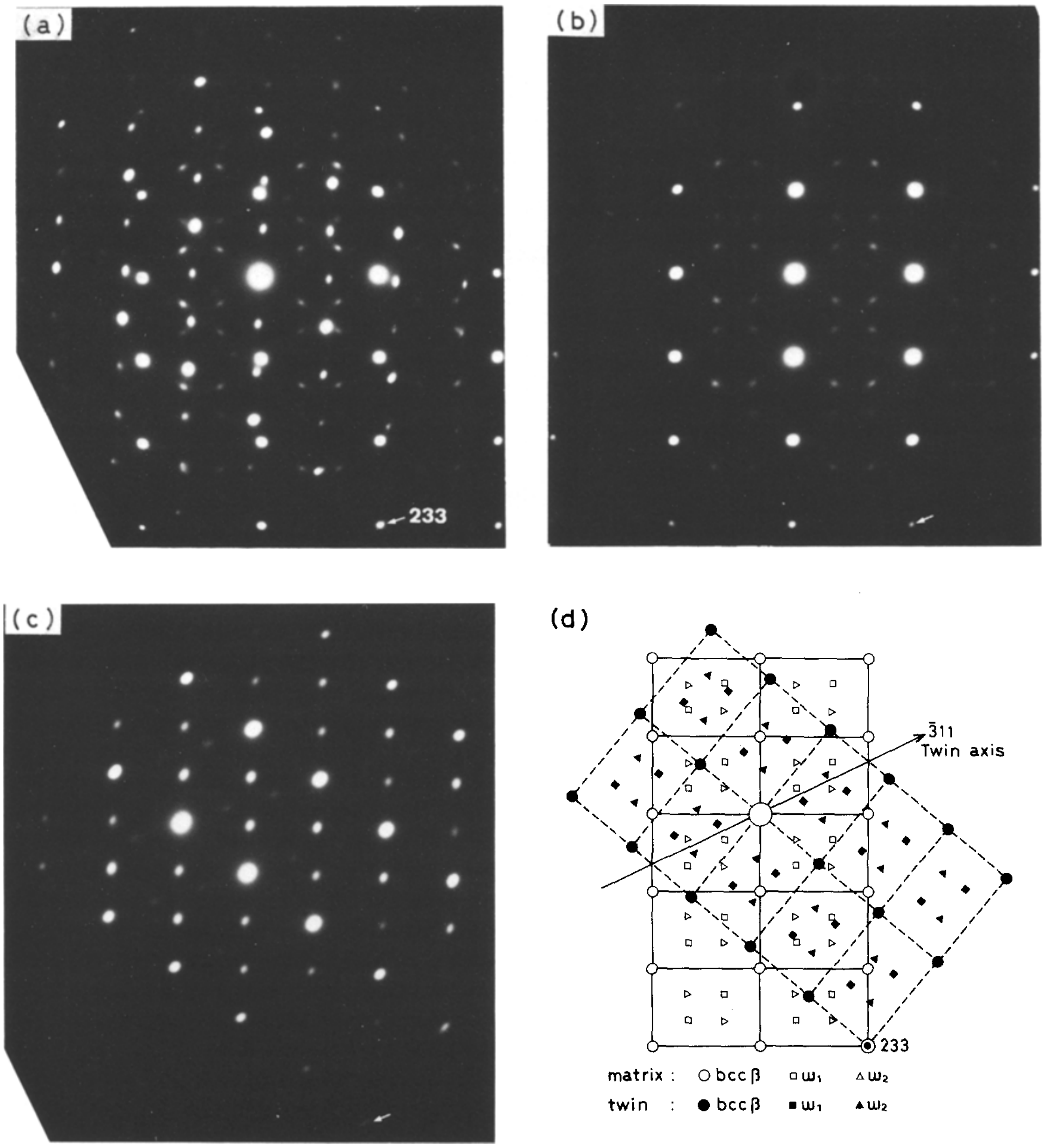

Figure 5 Selected area electron diffraction patterns taken from boundary region of a stress-induced product (a), β phase matrix (b), and the product (c) in a deformed Ti–10 wt % Cr alloy, (d) schematic diffraction pattern of (a).

strength $\sigma_{0.2}$ shows a minimum in the Ti–10 wt % Cr alloy, although tensile strength σ_B is independent of chromium content. Elongation to fracture is remarkably large in the Ti–8 wt % Cr and Ti–10 wt % Cr alloys. On the other hand, reduction of area is small in the Ti–8 wt % Cr alloy. Fig. 9 shows fractured surfaces of Ti–Cr alloys deformed at 300 K, showing dimple patterns independent of composition. Fig. 10 shows tensile properties of Ti–Cr alloys deformed at 77 K. Yield and tensile strength are lower in the Ti–Cr alloys accompanied by stress-induced ω transformation (Ti–8 wt % Cr) or mechanical twinning (Ti–10 wt % Cr and Ti–11.5 wt % Cr) than in the Ti–Cr alloys deformed by slip. Large elongation is obtained in the Ti–8 wt % Cr alloy. Fig. 11 shows fractured surfaces of Ti–Cr alloys deformed at 77 K. With increasing chromium content grain boundary facets appear significantly. The grain boundary fracture seems to result in small elongation and low reduction of area in higher chromium content alloys.

4. Discussion

Although ω phase was found about 30 years ago to be obtained not only by ageing but also by deformation of metastable β phase [5, 6], the mechanism of stress-induced ω formation is not well understood. It has recently been observed that stress-induced ω phase forms via $\{332\}\langle113\rangle$ mechanical twinning in unstable β Ti–Fe [10] and Ti–V [11] alloys. Namely, the reflections of a single variant of ω phase become preferentially distinct in a $\{332\}\langle113\rangle$ twin of β phase alloys slightly richer in alloy content than the minimum alloy content to suppress martensitic transformation during quenching. On the other hand, it has been generally recognized in many titanium alloys, such as Ti–V, Ti–Mo, Ti–Nb and Ti–Fe, that ω phase forms by ageing of metastable β phase [1–4], and $\{332\}\langle113\rangle$ mechanical twinning occurs by deformation of metastable β phase [12–20]. Therefore, plastic deformation modes in these alloys are expected to change from slip into ω transformation

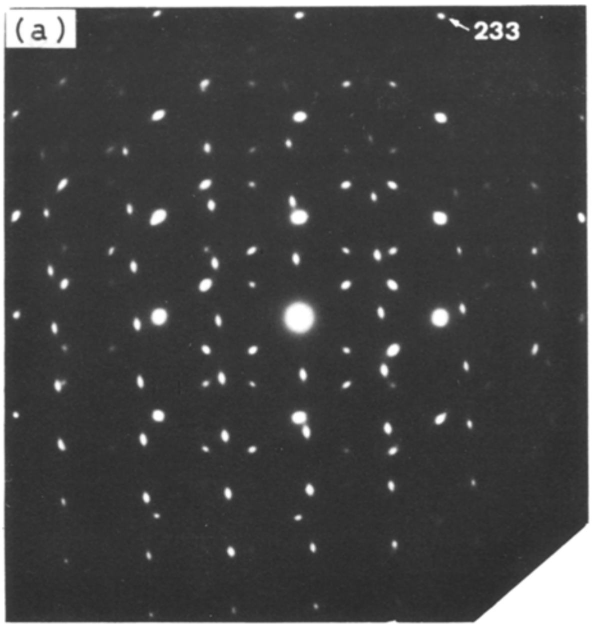

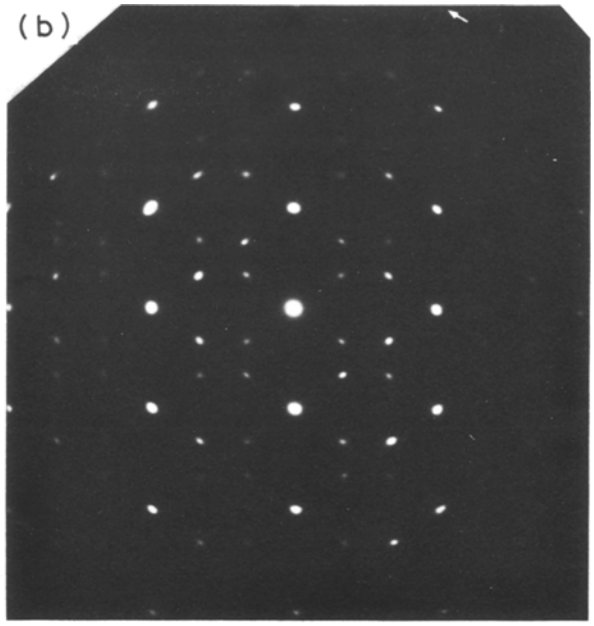

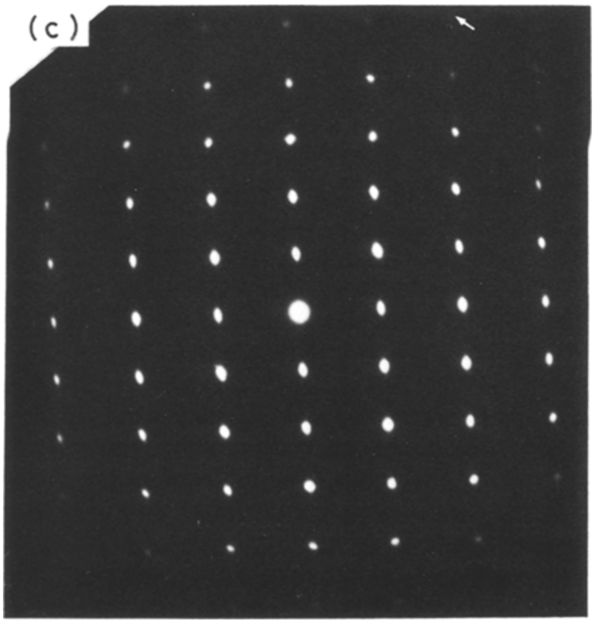

Figure 6 Selected area electron diffraction patterns taken from boundary region of a stress-induced product (a), β phase matrix (b), and the product (c) in a deformed Ti–8 wt % Cr alloy.

through {3 3 2} ⟨1 1 3⟩ mechanical twinning with decreasing stability of retained β phase. In the present experiments on Ti–Cr alloys the expected deformation modes described above were found as a function of composition. Especially, two variants of ω phase in the Ti–10 wt % Cr alloy show anisotropic population as shown in Fig. 5c, suggesting that the transition from {3 3 2} ⟨1 1 3⟩ twinning into ω transformation occurs continuously with a change of composition.

Conflicting results have been reported on deformation modes of β Ti–Mo alloys [8, 9, 11, 21] and no apparent stress-induced ω transformation has been detected in β Ti–Nb alloys [11]. However, the expected composition dependence of deformation modes seems to appear by controlling alloy composition, content of interstitial atoms such as oxygen or hydrogen and quenching rate, since stability of a retained β phase is significantly affected by these experimental conditions [8, 11, 22–25].

The intensity of (1 1 0) diffraction line in the as-quenched Ti–8, 10 or 13 wt % Cr plate is very weak in comparison with the predicted intensity of randomly oriented polycrystals. The cause may be ascribed to development of recrystallization texture. According to Ling *et al.* [26], Ti–V alloys showing identical composition dependence of deformation modes to β Ti–Cr alloys exhibit pronounced recrystallization textures {1 1 1} ⟨1 1 2⟩ + {1 1 2} ⟨1 2 4⟩. Development of the textures is consistent with the weak (1 1 0) diffraction lines in the as-quenched Ti–Cr alloys. It is apparent from Figs 2, 3 and 4 that the increase in intensity of (1 1 0) diffraction line by rolling is remarkably in the Ti–10 wt % Cr alloy deformed preferentially by {3 3 2} ⟨1 1 3⟩ twinning. This result can be explained by reorientation due to introduction of twelve different {3 3 2} ⟨1 1 3⟩ twinning systems.

It is accepted that ω phase of as-quenched β titanium alloys gives sharp reflections in low solute content alloys and diffuse reflections in high solute content alloys. To investigate the relation between the structural change of ω phase and plastic deformation modes for Ti–Cr alloys with different solute contents, (1 1 0) reciprocal lattice sections are compared in Fig. 12. We can see in this figure the following characteristics concerning the behaviour of the ω reflections. The appearance of the ω reflections changes continuously from sharp to diffuse with increasing chromium content. In addition, in the high chromium content alloys the diffuse reflections move away from the positions on lines joining b c c reflections, that is, the positions of the 0 0 0 1 and 0 0 0 2 reflections are displaced toward each other along ⟨1 1 1⟩ direction. In other words, this is incommensurate structure. Ratios of reciprocal space distances d^*_{0002}/d^*_{222} for the as-quenched Ti–Cr alloys are found to decrease with increasing chromium content, as shown in Fig. 13. Similar observations to this figure have been made for

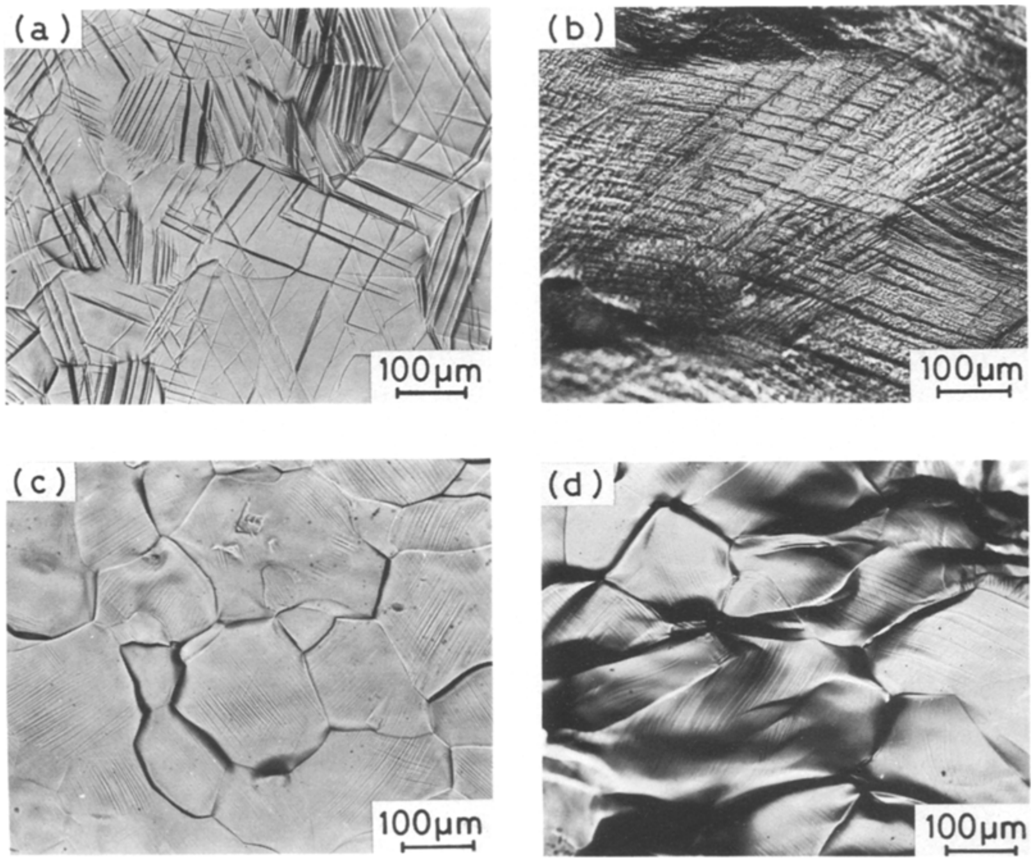

Figure 7 Optical micrographs of a Ti–10 wt % Cr alloy deformed in tension slightly (a) and fractured (b) and of a Ti–13 wt % Cr alloy deformed in tension (c) slightly and (d) fractured.

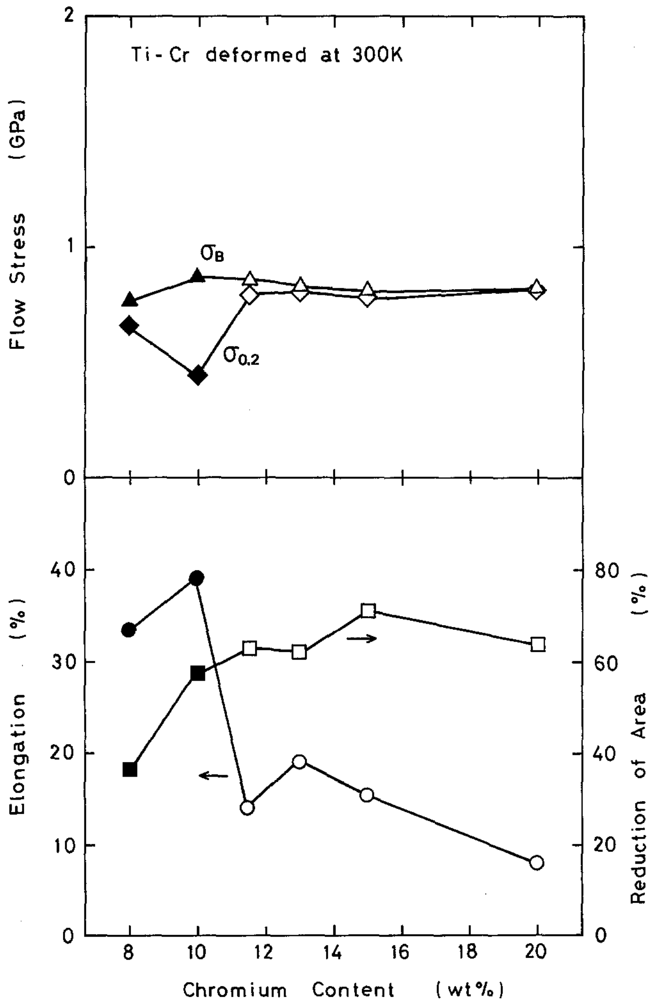

Figure 8 Composition dependence of tensile properties in Ti–Cr alloys deformed at 300 K.

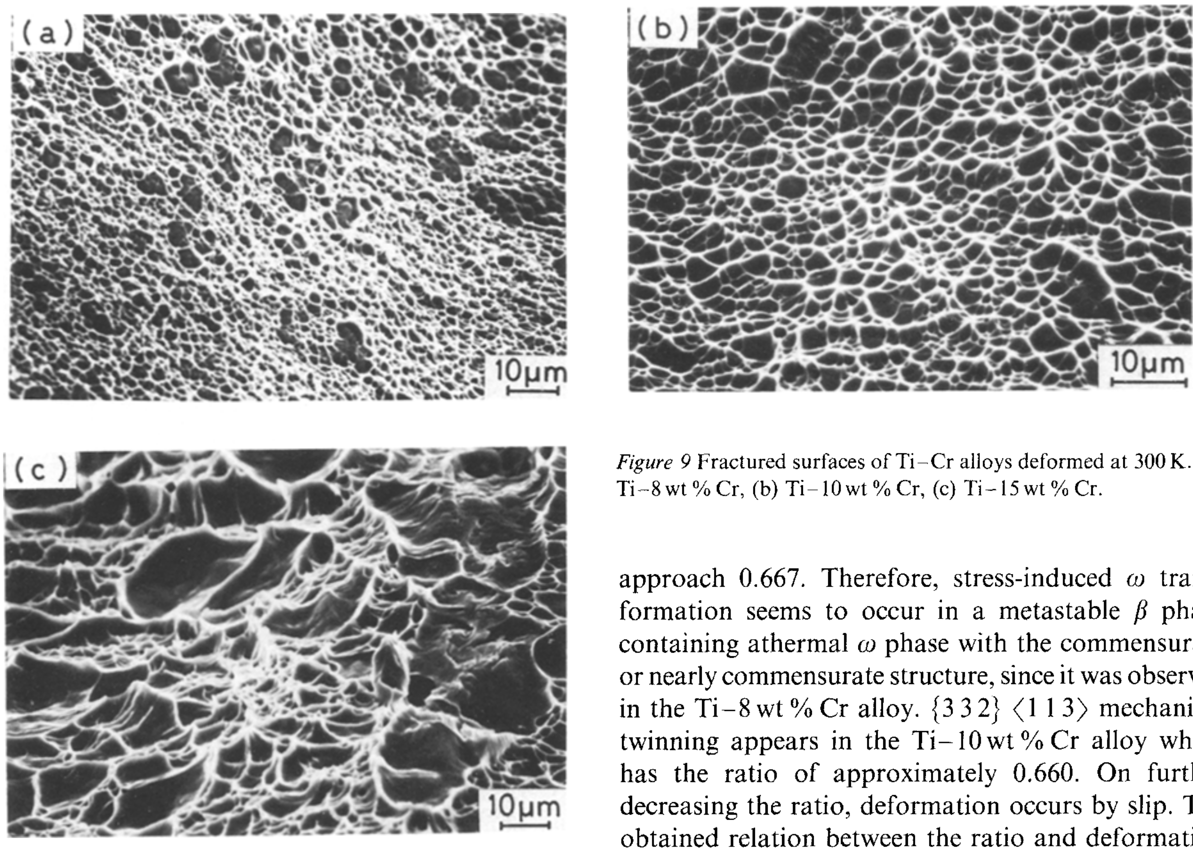

Figure 9 Fractured surfaces of Ti–Cr alloys deformed at 300 K. (a) Ti–8 wt % Cr, (b) Ti–10 wt % Cr, (c) Ti–15 wt % Cr.

Ti–V, Ti–Mo and Ti–Nb alloys [11]. The dotted line in Fig. 13 indicates the ideal ω structure with the ratio of 0.667, i.e. commensurate structure. With decreasing chromium content the ratio has a tendency to approach 0.667. Therefore, stress-induced ω transformation seems to occur in a metastable β phase containing athermal ω phase with the commensurate or nearly commensurate structure, since it was observed in the Ti–8 wt % Cr alloy. $\{332\}\langle 113\rangle$ mechanical twinning appears in the Ti–10 wt % Cr alloy which has the ratio of approximately 0.660. On further decreasing the ratio, deformation occurs by slip. The obtained relation between the ratio and deformation modes in the Ti–Cr alloys holds true in Ti–V, Ti–Mo and Ti–Fe alloys in the previous paper [11]. Recently, Terauchi *et al.* [27] have shown in aged β Ti–Mo alloys that there exists a discontinuous change from the commensurate to incommensurate structure at the

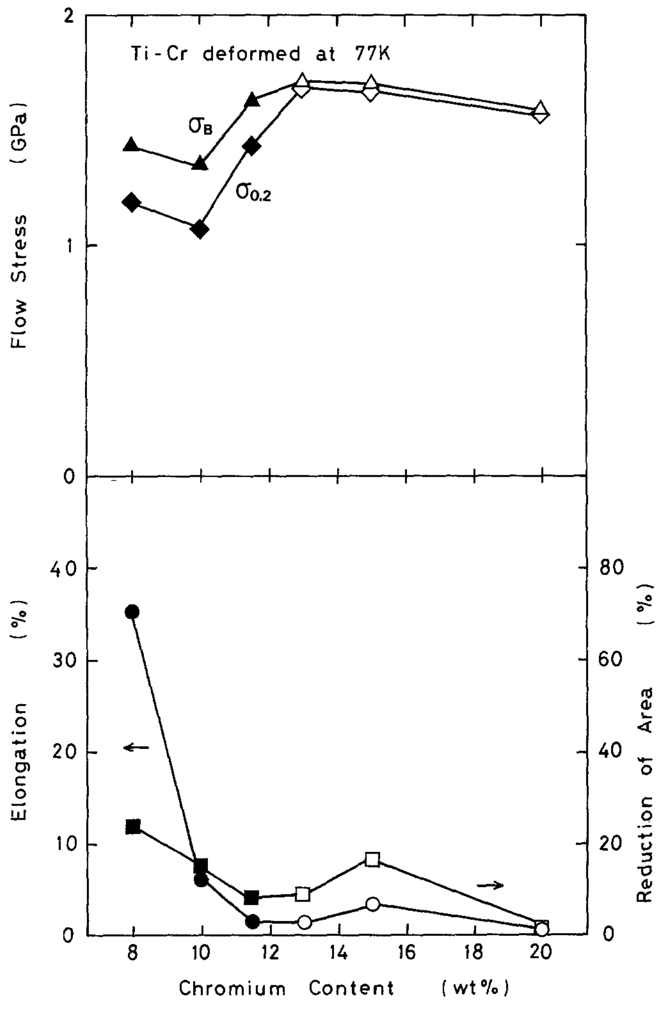

Figure 10 Composition dependence of tensile properties in Ti–Cr alloys deformed at 77 K.

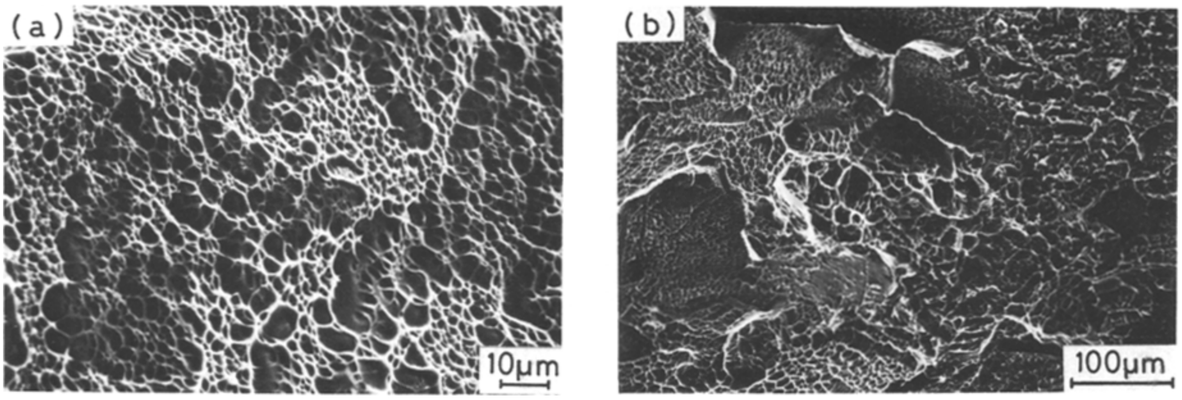

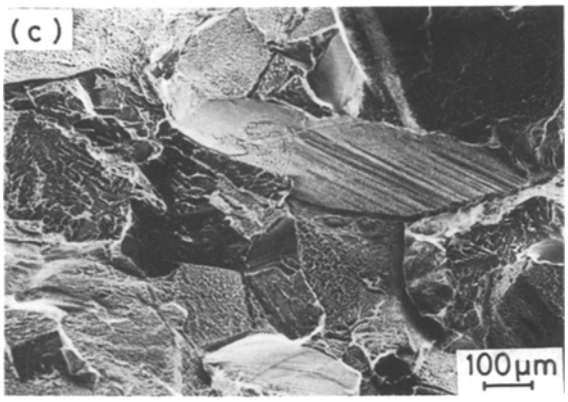

Figure 11 Fractured surfaces of Ti–Cr alloys deformed at 77 K. (a) Ti–8 wt % Cr, (b) Ti–11.5 wt % Cr, (c) Ti–20 wt % Cr.

critical composition of Ti–18 wt % Mo. On the other hand, Hida *et al.* [8] observed the incommensurate structure in a quenched Ti–14 wt % Mo alloy. The present authors [11] have also observed the incommensurate structure in a quenched Ti–Mo alloys with compositions between 11 and 20 wt % Mo. These observations suggest that the structure of ω phase in quenched Ti–Mo alloys changed by ageing from the incommensurate to commensurate at the composition

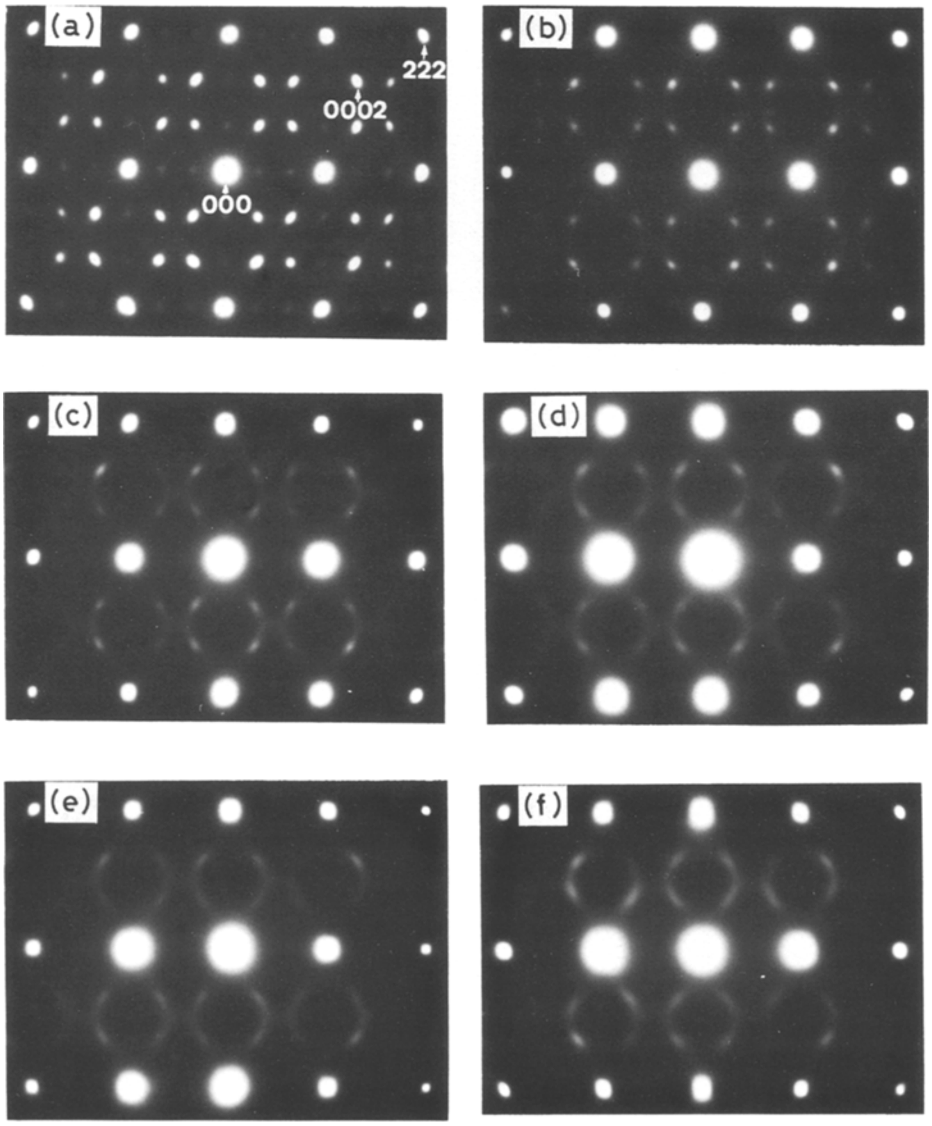

Figure 12 Selected area electron diffraction patterns of as-quenched Ti–Cr alloys showing the (1 1 0) reciprocal lattice section. (a) Ti–8 wt % Cr, (b) Ti–10 wt % Cr, (c) Ti–11.5 wt % Cr, (d) Ti–13 wt % Cr, (e) Ti–15 wt % C, (f) Ti–20 wt % Cr.

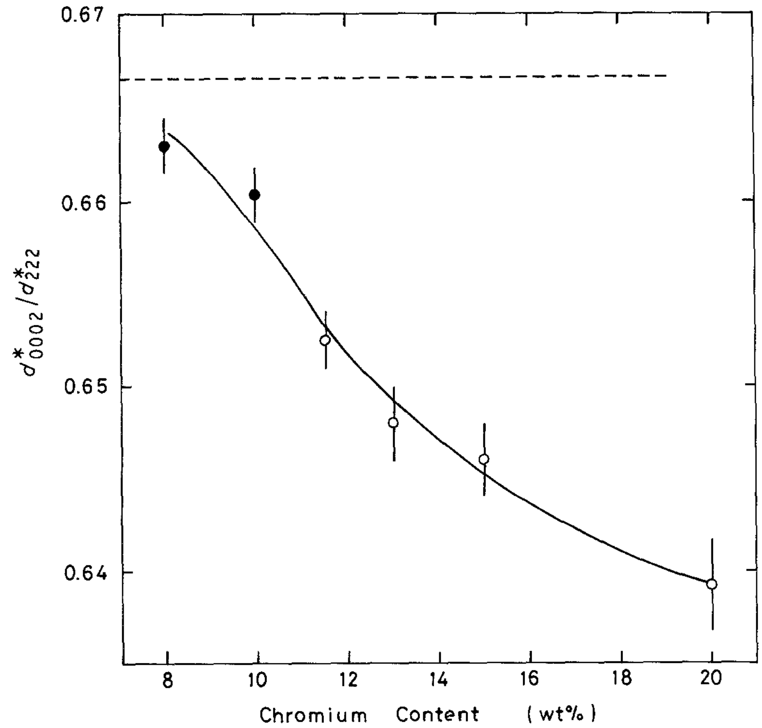

Figure 13 Composition dependence of ratio of reciprocal space distance d^*_{0002}/d^*_{222} for the as-quenched Ti–Cr alloys.

range between 11 and 18 wt % Mo. This composition range is in good agreement with the composition range where {3 3 2} ⟨1 1 3⟩ twinning occurs [11]. Thus, the occurrence of {3 3 2} ⟨1 1 3⟩ twinning is closely related to the stability of β phase concerning decomposition to ω phase.

5. Summary

Three types of plastic deformation modes, i.e. stress-induced phase transformation, {3 3 2} ⟨1 1 3⟩ mechanical twinning and slip, were found to operate during deformation of retained β phase in β-eutectoid Ti–Cr alloys. Stress-induced ω phase forms in a {3 3 2} ⟨1 1 3⟩ twin of the most unstable β phase having minimum chromium content required to suppress martensitic transformation. Anisotropy in population of ω phase variants in a {3 3 2} ⟨1 1 3⟩ twin decreases with increasing chromium content. Slip occurs during deformation of higher chromium content alloys. Composition dependence of deformation modes is related to the stability of β phase concerning decomposition to ω phase. Enhanced ductility is obtained in as-quenched Ti–Cr alloys accompanied by ω phase transformation or {3 3 2} ⟨1 1 3⟩ twinning during deformation.

Acknowledgements

We would like to thank Professor Emeritus Z. Nishiyama for his encouragement. We also acknowledge Osaka Titanium Co., Ltd. for the supply of high purity titanium.

References

1. B. S. HICKMAN, *J. Mater. Sci.* **4** (1969) 554.
2. S. L. SASS, *J. Less-Common Metals* **28** (1972) 157.
3. Z. NISHIYAMA, *Bull. Jpn. Inst. Met.* **14** (1975) 499.
4. S. K. SIKKA, Y. K. VOHRA and R. CHIDAMBARAM, *Prog. Mater. Sci.* **27** (1982) 245.
5. F. R. BROTZEN, E. L. HARMON and A. R. TROIANO, *Trans. AIME* **203** (1955) 413.
6. YU. A. BAGARYATSKIJ, T. V. TAGUNOVA and G. I. NOSOVA, *Problemy Metallovedenija i Fisiki Metallov, Moscow* **5** (1958) 210.
7. T. S. KUAN, R. R. AHRENS and S. L. SASS, *Metall. Trans.* **6A** (1975) 1767.
8. M. HIDA, E. SUKEDAI, C. HENMI, K. SAKAUE and H. TERAUCHI, *Acta Metall.* **30** (1982) 1471.
9. J. M. SILCOCK, *ibid.* **6** (1958) 481.
10. S. HANADA, T. YOSHIO and O. IZUMI, *J. Mater. Sci.* **21** (1986) 866.
11. S. HANADA and O. IZUMI, *Metall. Trans.* in press.
12. M. J. BLACKBURN and J. A. FEENEY, *J. Inst. Met.* **99** (1971) 132.
13. J. A. ROBERTSON, S. FUJISHIRO, V. S. ARUNACHALAM and C. M. SARGENT, *Metall. Trans.* **5** (1974) 2317.
14. G. CARTER, H. M. FLOWER, G. M. PENNOCK and D. F. WEST, *J. Mater. Sci.* **12** (1977) 2149.
15. M. OKA and Y. TANIGUCHI, *J. Jpn. Inst. Met.* **42** (1978) 814.
16. O. A. YELKINA and R. M. LERINMAN, *Phys. Met. Metall.* **45** (1979) 78.
17. M. HIDA, E. SUKEDAI, Y. YOKOHARI and A. NAGASAWA, *J. Jpn. Inst. Met.* **44** (1980) 436.
18. S. HANADA and O. IZUMI, *Metall. Trans.* **11A** (1980) 1447.
19. S. HANADA, A. TAKEMURA and O. IZUMI, *Trans. Jpn. Inst. Met.* **23** (1982) 507.
20. S. HANADA, M. OZEKI and O. IZUMI, *Metall. Trans.* **16A** (1985) 789.
21. R. M. WOOD, *Acta Metall.* **11** (1963) 907.
22. N. E. PATON and J. C. WILLIAMS, *Scripta Metall.* **7** (1973) 647.
23. J. C. WILLIAMS, D. de FONTAINE and N. E. PATON, *Metall. Trans.* **4** (1973) 2701.
24. O. BUCK, D. O. THOMPSON, N. E. PATON and J. C. WILLIAMS, in Proceedings of the 5th International Conference on Internal Friction and Ultrasonic Attenuation in Crystalline Solids, Aachen, August 1973, (Springer, Berlin 1975), p. 451.
25. T. S. LUHMAN and A. E. CURZON, *J. Mater. Sci.* **7** (1972) 710.
26. F. W. LING, E. A. STARKE Jr and B. G. LEFEVRE, *Metall. Trans.* **5** (1974) 179.
27. H. TERAUCHI, K. SAKAUE and M. HIDA, *J. Phys. Soc. Jpn.* **50** (1981) 3932.

Received 2 January
and accepted 11 February 1986